

Reverse Engineering of Proteasomal Translocation Rates

D.S. Goldobin,^{1,2} M. Mishto,^{3,4} K. Textoris-Taube,⁴ P.M. Kloetzel,⁴ and A. Zaikin⁵

¹Department of Physics, University of Potsdam, Postfach 601553, D-14415 Potsdam, Germany

²Department of Theoretical Physics, Perm State University, 15 Bukireva str., 614990, Perm, Russia

³CIG, University of Bologna, I-40126 Bologna, Italy

⁴Institute of Biochemistry, Charité, Humboldt University, Mombjousstr. 2, 10117 Berlin, Germany

⁵Department of Mathematical & Biological Sciences, University of Essex, CO4 3SQ, Colchester, UK

We address the problem of proteasomal protein translocation. Proteasomes are important for all aspects of the cellular metabolism but the mechanism of protein transport remains unknown. We introduce a new stochastic model of the proteasomal transport. We account for the protein translocation and the topology of the positioning of cleavage centers of a proteasome from first principles. We show by test examples and by a comparison with experimental data that our model allows reconstruction of the translocation rates from mass spectroscopy data on digestion patterns and can be used to investigate the properties of transport in different experimental set-ups. Finally we design an experimental set-up for a synthetic polypeptide with a periodic sequence of amino acids which enables more reliable determination of translocation rates.

PACS numbers: 05.40.-a, 87.15.R-, 87.19.xv

A macromolecular complex, the proteasome, is the central molecular machine for the degradation of intracellular proteins [1]. Proteasomes have a pivotal role in antigen processing producing epitopes for an immune system [2]. They exist in cells as the free proteolytically active core, the barrel-shaped 20S proteasome (Fig.1), and as associations of this core with regulatory complexes (PA700 or PA28) at its ends [3]. Here we consider *in vitro* proteasomal digestion widely used in molecular biology and immunology to investigate proteasomes.

A protein enters the proteasome and is transported into the central chamber where it is cleaved into fragments by one of the cleavage terminals arranged along two rings. Fragments of the protein produced are removed through proteasome gates. Peculiarities of the translocation rates can qualitatively affect the expression of the specific fragment, *e.g.*, an epitope, because an altered transport changes time of being near the cleavage terminal, *i.e.*, conditions of cleavage. Moreover, impairment of proteasomal degradation, probably due to transport malfunction, might contribute to the pathology of various neurodegenerative conditions [4].

The mechanism of protein translocation remains unknown. It is also unknown whether transport properties will be different for different proteasome types (constitutive or immuno-), with/without different regulatory complexes, and with different experiment conditions (concentration ratios, temperature, *etc.*). Only a few papers address the translocation problem but these are either based on semi-phenomenological descriptions of uptake and translocation of the protein [5, 6, 7] or they suggest a transport mechanism hypothesis not yet verified by experiment [8]. In contrast to these approaches, here we introduce a stochastic model which allows one to *reconstruct* the translocation rates and cleavage probabilities from mass spectroscopy (MS) data on

digestion patterns. Using this model we consider degradation of (i) relatively short synthetic polypeptides and (ii) long proteins with a periodic sequence of amino acids (aa). Reconstructed features of a specific proteasome type can be used for prediction of the fragment expression.

In our model of the process of protein transport and degradation by the proteasome (see Fig.1) we assume that:

- (1) The probability of the protein shift by one aa during the time unit into the proteasome (to the right in Fig.1) is assumed to depend only on the length x of the protein forward end beyond the active sites nearest to the proteasome chamber entrance used for protein infiltration (the left ones in Fig.1); this probability is given by the translocation rate function (TRF) $v(x) \equiv v_x$. The backward motions of the entering strand are neglected. These assumptions do not impose significant restrictions

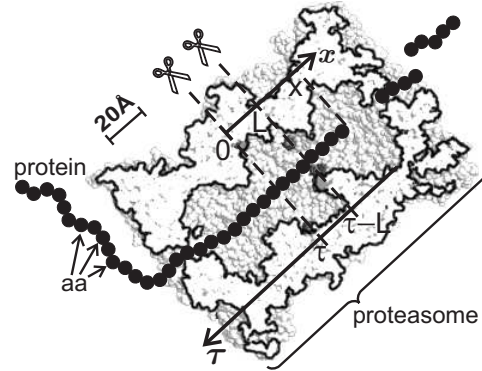


FIG. 1: Infiltration of a protein strand into the 20S proteasome: The scissors mark the positions of active sites rings at $x = 0$ and $x = L$; the cleavage occurs via the attaching-detaching of the protein to active sites (dark-grey color).

on the physical mechanism of the translocation process: they are valid for the thermal drift in a tilted spatially-periodic potential [9] as well as for the ratchet effect [8], *etc.* The TRFs of different proteasome species (20S, 26S, \pm PA28 [3]) may differ.

(2) When the protein strand is close to the active site, the probability of cleavage during the unit time depends on the sequence of aa nearest to the peptide bond cleaved [10]. For the given protein, this conditional cleavage probability (CCP), $\gamma(\tau) \equiv \gamma_\tau$, is a function of the bond number τ (Fig.1); later on we use τ as a *time-like variable*.

(3) The peptides (cleaved parts of the protein degraded) leave the chamber through proteasome gates. Due to their mobility being higher in comparison to that of the protein, processed peptides leave the chamber quick enough to neglect both their possible further splitting and their influence on the protein transport.

Next we describe the evolution of the distribution $w(x|\tau)$ of the length x of the protein forward end beyond the first ring of the active sites at the discrete “time moment” τ . We measure x in aa. Accounting for the gains to and the losses of $w(x|\tau)$ during the shift of the protein chain for one aa, *i.e.*, the transition $\tau \rightarrow \tau + 1$, one finds the master equations (for the detailed derivation see [11])

$$w(1|\tau+1) = \sum_{x=1}^L \frac{\gamma_\tau w(x|\tau)}{v_x + \gamma_\tau} + \sum_{x=L+1}^{\infty} \frac{\gamma_\tau w(x|\tau)}{v_x + \gamma_\tau + \gamma_{\tau-L}} + \frac{\gamma_\tau}{v_L + \gamma_\tau} \sum_{x=L+1}^{\infty} \frac{\gamma_{\tau-L} w(x|\tau)}{v_x + \gamma_\tau + \gamma_{\tau-L}}; \quad (1)$$

$$w(L+1|\tau+1) = \frac{v_L}{v_L + \gamma_\tau} \times \left[w(L|\tau) + \sum_{x=L+1}^{\infty} \frac{\gamma_{\tau-L} w(x|\tau)}{v_x + \gamma_\tau + \gamma_{\tau-L}} \right]; \quad (2)$$

$x \neq 1, x \neq L+1$:

$$w(x|\tau+1) = \frac{v_{x-1} w(x-1|\tau)}{v_{x-1} + \gamma_\tau + \Theta(x-L-1)\gamma_{\tau-L}}. \quad (3)$$

Here L is the distance between the rings of active sites (Fig.1), $x = 1, 2, 3, \dots, M$ and $\tau = 1, 2, 3, \dots, M-1$, where M is the length of the protein, and the Heaviside function $\Theta(x) = \begin{cases} 0 & \text{for } x < 0, \\ 1 & \text{for } x \geq 0. \end{cases}$ Eqs.(1-3) form a linear map

$$w(x|\tau+1) = \sum_{y=1}^{\infty} \mathcal{L}_{xy}(\tau) w(y|\tau). \quad (4)$$

First we consider degradation of *short* (25–50 aa) *synthetic polypeptide*, the most common situation for *in vitro* experiments. Here we start at $\tau = 1$ with $w(x|\tau = 1) = \delta_{x,1}$ and evaluate Eq.(4) till the last $\tau = M - 1$. With $w(x|\tau)$ known for $\tau = 1, 2, \dots, M$, one may evaluate the cleavage pattern, *i.e.* the amount $Q(m, n)$ of the peptide (n, m) (where n and m denote the sequence position of

the peptide within the initial substrate) generated after a single polypeptide processing,

$$Q(\tau_1, \tau_2) = \delta_{\tau_1, M} w(\tau_1 + L - \tau_2 + 1|M) + \frac{\gamma_{\tau_1} w(\tau_1 - \tau_2 + 1|\tau_1)}{v_{\tau_1 - \tau_2 + 1} + \gamma_{\tau_1} + \Theta(\tau_1 - \tau_2 - L)\gamma_{\tau_1 - L}} + \frac{\delta_{\tau_1 - \tau_2 + 1, L} \gamma_{\tau_1}}{v_L + \gamma_{\tau_1}} \sum_{x=L+1}^M \frac{\gamma_{\tau_1 - L} w(x|\tau_1)}{v_x + \gamma_{\tau_1} + \gamma_{\tau_1 - L}} + \Theta(M - \tau_1 - L) \frac{\gamma_{\tau_1} w(\tau_1 + L - \tau_2 + 1|\tau_1 + L)}{v_{\tau_1 + L - \tau_2 + 1} + \gamma_{\tau_1 + L} + \gamma_{\tau_1}}, \quad (5)$$

here $1 \leq \tau_2 \leq \tau_1 \leq M$ (details in [11]). Since the protein may be cleaved starting both from the C- and from the N-terminal, the final digestion pattern is given by

$$Q_{\text{fin}}(\tau_1, \tau_2) = P_N Q_N(\tau_1, \tau_2) + P_C Q_C(M - \tau_2 + 1, M - \tau_1 + 1). \quad (6)$$

The subscripts indicate which terminal goes first, P_N and $P_C = 1 - P_N$ are the probabilities of the degradation starting from the corresponding end. Generally, $v_N(x)$ and $v_C(x)$ may be slightly different, but here we neglect this difference. Note that a product length distribution $P(x)$ (often used in the literature [12]) is then the convolution $P(x) = \sum_{\tau=1}^{M-x} Q(\tau, \tau - x)$.

The digestion pattern $Q_{\text{fin}}(\tau_1, \tau_2)$ is a functional of the TRF $v(x)$ and the CCP $\gamma(\tau)$. Utilizing MS data on

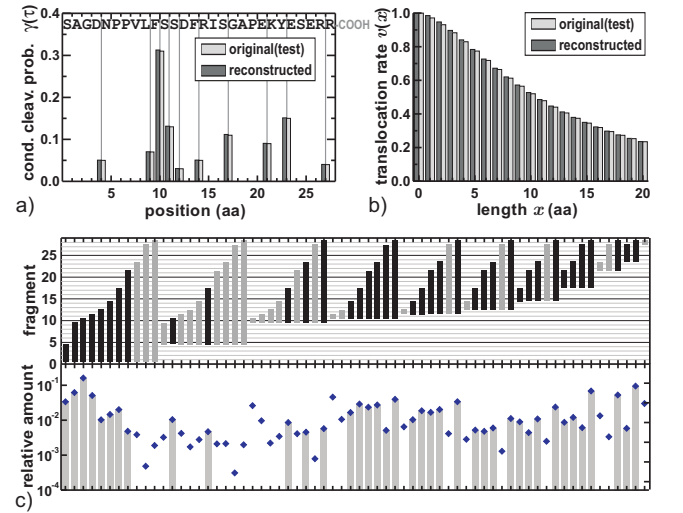


FIG. 2: Test — Reconstruction of the translocation function $v(x)$ and the conditional cleavage probability $\gamma(\tau)$ for the 28mer peptide Kloe 320 [13][but with unreal values $\gamma(\tau)$]. a) the conditional cleavage probabilities and the aa sequence; b) the translocation rate function; c) the upper plot presents a set of digestion fragments (black bars: fragments utilized for the reconstruction, gray bars: not utilized), and the lower plot presents the amount of the corresponding fragment (diamonds: the reconstructed values Q_{fin} , gray bars: the values of Q utilized for the reconstruction).

the digestion pattern, one can determine nonzero values of $\gamma(\tau)$ (*i.e.* positions of possible cleavage) and minimize the mismatch between $Q_{\text{fin}}(\tau_1, \tau_2)$ and MS data $\hat{Q}(\tau_1, \tau_2)$ over $v(x)$, the nonzero values of $\gamma(\tau)$, and P_N in order to *reconstruct* them. Expecting the function $v(x)$ to be smooth, we parameterize appropriate approximate functions as

$$v_{\text{app}}(x) = v_0 e^{-\frac{A_2^2}{\sqrt{A_1^2+x}} + \frac{A_2^2}{|A_1|} - A_3^2(\sqrt{A_1^2+x} - |A_1|)} \quad (7)$$

Note, $v(x)$ and $\gamma(\tau)$ are defined up to the constant multiplier, which should be determined from the degradation rate in real time, but not from the digestion pattern.

In order to verify the robustness of the reverse engineering procedure, numerous tests have been performed. A typical test presented in Fig.2 has been performed as follows. For given $v(x)$ [not generic for v_{app} , *i.e.*, the used function $v(x)$ cannot be perfectly fitted with the expression (7)] and $\gamma(\tau)$ the digestion pattern $Q(\tau_1, \tau_2)$ has been evaluated. The result has been perturbed by the noise $\hat{Q}_{\tau_1\tau_2} = Q_{\tau_1\tau_2} + 10^{-4}R_{\tau_1,\tau_2}\sqrt{Q_{\tau_1,\tau_2}}$, where R_{τ_1,τ_2} are independent random numbers uniformly distributed in $[-1, 1]$. The information about 1mer and 2mer fragments and fragments which relative amount is less than $5 \cdot 10^{-3}$ has been omitted as being hardly detectable in experiments [14]. Resulting $\hat{Q}_{\tau_1\tau_2}$ has been used for the reconstruction of $v(x)$ and $\gamma(\tau)$. The original and reconstructed data for $\gamma(\tau)$ (Fig.2a) and $v(x)$ (Fig.2b) are in a good agreement. The reconstructed $P_N = 0.49$ against original $P_N = 0.50$.

Fig.3 presents the results of the reverse engineering from the experimental (*in vitro*) digestion pattern for the 28mer Kloe 258, which is the sequence 101–128 aa

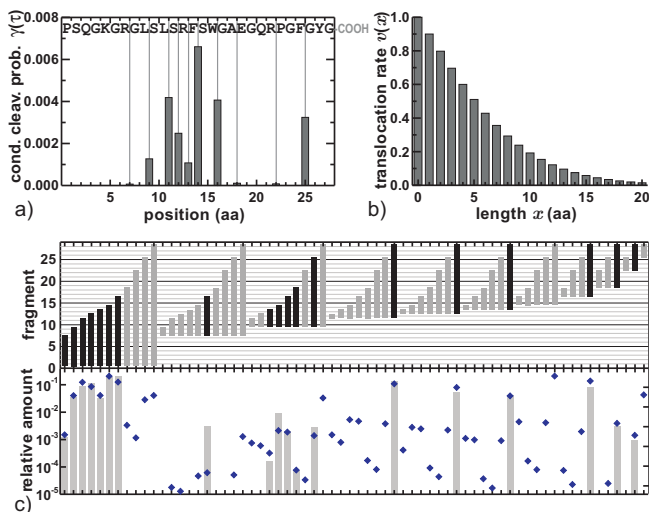


FIG. 3: Experiment — Reconstruction of the translocation function $v(x)$ and the conditional cleavage probabilities $\gamma(\tau)$ for the 28mer peptide Kloe 258 degraded by a 20S proteasome; $P_N = 54\%$. (For description see caption to Fig.2.)

of human myelin basic protein, degraded by 20S proteasomes purified from lymphoblastoid cell lines, which express mainly the immunoproteasome (for materials and methods see [13], [17]). The TRF $v(x)$ appears to be monotonically decaying; the reconstructed probability of the degradation starting from the N-terminal $P_N = 54\%$, meaning the degradation from the two ends was almost equally probable in this case.

The suggested reconstruction method has some limitations. The reconstruction procedure for short polypeptides is very sensitive to measurement inaccuracy. Though the whole information on $Q(\tau_1, \tau_2)$ is not needed, the number of nonzero values of $Q(\tau_1, \tau_2)$ required for a reliable (tolerant to noise) reconstruction is at least the twice number of reconstructed parameters, *i.e.* $2 \times \left(\left[\begin{smallmatrix} \text{number of positions} \\ \text{of potential cleavage} \end{smallmatrix} \right] + \left[\begin{smallmatrix} \text{number of para-} \\ \text{meters of } v_{\text{app}} \end{smallmatrix} \right] + 1 \right)$. For Kloe 258 the number of trustworthy and utilized values of $\hat{Q}(\tau_1, \tau_2)$ is 19 instead of the required $2 \times (10 + 3 + 1) = 28$ (see Fig.3), it is a bit greater than the number of the unknown parameters, *i.e.*, 14. Hence, more accurate and comprehensive MS data on the digestion pattern are required. Additionally, for short polypeptides the finishing stage of the degradation is relatively important, while in this stage the translocation rate is affected by the edge effects (the backward end of the polypeptide gets inside the proteasome chamber) and is not the same as for the remainder of the polypeptide.

All these limitations may be overcome in the experimental set-up designed for future study of the proteasome TRF. For this a *long polypeptide with a T-periodic aa sequence*: $\gamma(\tau) = \gamma(\tau + T)$ should be digested. Here “long” means one may neglect the pe-

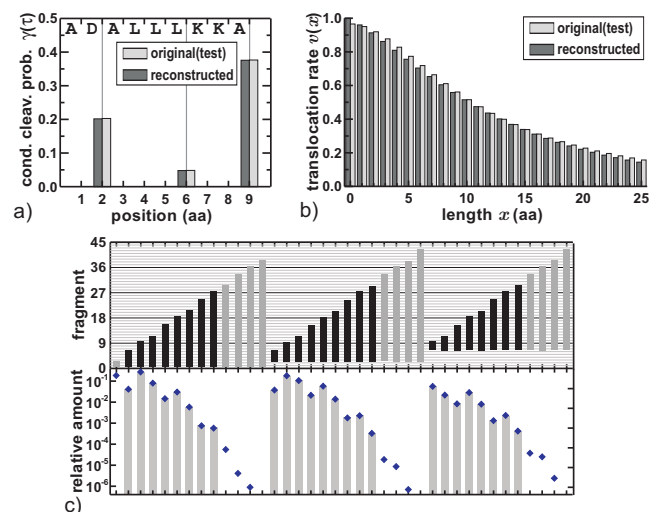


FIG. 4: Test — Reconstruction of the translocation function $v(x)$ and the conditional cleavage probabilities $\gamma(\tau)$ for a 9-periodic polypeptide with the cleavage positions 2, 6, 9. (For description see caption to Fig.2.)

cularities of the edge effects of the degradation, and $M \gg T$. For the given direction of the degradation, *e.g.*, starting with the N-terminal, we are looking for the establishing T -periodic in τ solution $w_{N,T}(x|\tau) = w_{N,T}(x|\tau - T)$ to Eq.(4). The fragment (n, m) is identical to the one $(n + kT, m + kT)$, where k is integer; therefore $Q_N(m, n)$ may be chosen to make contribution to $Q_N(m - n + (n \bmod T), n \bmod T)$. Hence, for the digestion pattern one obtains (details in [11])

$$Q_{N,T}(\tau_1, \tau_2) = \frac{1}{T} \left[\frac{\gamma_{\tau_1} w_{N,T}(\tau_1 - \tau_2 + 1|\tau_1)}{v_{\tau_1 - \tau_2 + 1} + \gamma_{\tau_1} + \Theta(\tau_1 - \tau_2 - L)\gamma_{\tau_1 - L}} + \frac{\delta_{\tau_1 - \tau_2 + 1, L} \gamma_{\tau_1}}{v_L + \gamma_{\tau_1}} \sum_{x=L+1}^{\infty} \frac{\gamma_{\tau_1 - L} w_{N,T}(x|\tau_1)}{v_x + \gamma_{\tau_1} + \gamma_{\tau_1 - L}} + \frac{\gamma_{\tau_1} w_{N,T}(\tau_1 + L - \tau_2 + 1|\tau_1 + L)}{v_{\tau_1 + L - \tau_2 + 1} + \gamma_{\tau_1 + L} + \gamma_{\tau_1}} \right] \quad (8)$$

(here $1 \leq \tau_2 \leq T$ and $\tau_1 \geq \tau_2$).

To treat the degradation process starting with the C-terminal, one has (i) to perform the transformation $\gamma(\tau) \rightarrow \gamma(T - \tau)$, (ii) evaluate Eq.(4) with the new $\gamma(\tau)$ like for the N-case, but assuming $Q_C(m, n|\tau)$ to make contribution to $Q_C(m \bmod T, n - m + (m \bmod T))$. Instead of (6), the result is

$$Q_{\text{fin}}(\tau_1, \tau_2) = P_N Q_{N,T}(\tau_1, \tau_2) + P_C Q_{C,T}(T - \tau_2, T - \tau_1).$$

Matching $Q_{\text{fin}}(m, n)$ to the MS data one can reconstruct $v(\tau)$, $\gamma(\tau)$, and P_N . For a test we have used the cleavage map of the degradation of yeast enolise-1 by human erythrocyte proteasome [15]. Looking at its subsequence 331–348 aa

...|ATAIEKKA|AD|ALLL|KV|NQ|...-COOH

(vertical stripes mark the positions of experimentally observed cleavages), one may expect the case, where the underlined subsequence is followed not by KV, but by KKA..., and the periodic sequence is

AD|ALLL|KKA|...|AD|ALLL|KKA|...|AD|ALLL|KKA-COOH,

to be realistic. For such a sequence a test like the one in Fig.2 (but with much stronger dithering: $\tilde{Q}_{\tau_1 \tau_2} = Q_{\tau_1 \tau_2} + 2 \cdot 10^{-3} R_{\tau_1, \tau_2} \sqrt{Q_{\tau_1, \tau_2}}$) is presented in Fig.4. Due to the small number of unknown parameters the reconstruction procedure is rather tolerant to measurement inaccuracy and does not require information on a large number of digestion fragments (the most easily detectable fragments are enough).

In summary, we have proposed a model of the degradation of proteins by the proteasome which allows one to *reconstruct* the proteasomal transport function. The model is applicable to the broad variety of hypothetically possible translocation mechanisms [8, 9]. We have tested a model for relatively short (25–50mers) synthetic

polypeptides as the most common case for *in vitro* experiments and suggested an experimental set-up for long periodic polypeptides.

Earlier, in [16], we have described how peculiarities of the translocation function may lead to the multimodality of the fragment length distribution even for $\gamma(\tau) \equiv \text{const}$. Here we have shown that the amount of each digestion fragment is not only determined by the cleavage map of the substrate but is also crucially affected by nonuniformity of the translocation rate. The proposed methodology can be used in extensive analysis of already available MS data for the 20S proteasomes and its associations with different regulatory complexes and under different experimental conditions, hence, giving insight into the mystery of the protein translocation mechanism inside the proteasome. Such an analysis can elucidate also the unanswered question whether there is some preference for starting the degradation with the N- or C-terminal of the protein, and how this preference is quantitatively affected by regulatory complexes. Moreover, hopefully, testing theoretical results by comparison to experimental data may stimulate new experiments as suggested in this letter for the case of the periodic polypeptide.

We thank S. Witt for fruitful discussions. The work was supported by grants of the VW-Stiftung, PROTEOMAGE – European Commission (FP6), the BRHE program, and the foundation “Perm Hydrodynamics”.

-
- [1] K. L. Rock *et al.*, Cell **78**, 761 (1994).
 - [2] P. M. Kloetzel, Nat. Rev. Mol. Cell. Biol. **2**, 179 (2001).
 - [3] N. Tanahashi *et al.*, J. Biol. Chem. **275**, 14336 (2000).
 - [4] D. C. Rubinsztein, Nature **443**, 780 (2006); M. Mishto *et al.*, CNSA-MC **7**, 236 (2007).
 - [5] H. G. Holzhütter and P. M. Kloetzel, Biophys. J. **79**, 1196 (2000).
 - [6] B. Peters *et al.*, J. Mol. Biol. **318**, 847 (2002).
 - [7] F. Luciani *et al.*, Biophys. J. **88**, 2422 (2005).
 - [8] A. Zaikin and T. Pöschel, Europhys. Lett. **69**, 725 (2005).
 - [9] P. Reimann *et al.*, Phys. Rev. Lett. **87**, 010602 (2001).
 - [10] S. Tenzer *et al.*, Cell. Mol. Life Sci. **62**, 1025 (2005).
 - [11] See Auxiliary Materials below for the detailed derivation of the master equation and expressions for cleavage patterns.
 - [12] A. F. Kisselev, T. N. Akopian, and A. L. Goldberg, J. Biol. Chem. **273**, 1982 (1998).
 - [13] M. Mishto *et al.*, J. Mol. Biol. **377**, 1607 (2008).
 - [14] A. Kohler *et al.*, Mol. Cell. **7**, 1143 (2001).
 - [15] A. K. Nussbaum *et al.*, Immunogenetics **53**, 87 (2001).
 - [16] A. Zaikin *et al.*, Biophys. Rev. Lett. **1**, 375 (2006).
 - [17] The data are taken for the time moment when 9% of the initial substrate has been degraded, *i.e.* the second proteasomal reprocessing of digestion products is negligible.

AUXILIARY MATERIALS

DERIVATION OF THE MASTER EQUATION

Within the frameworks of the model we propose in the letter for the process of proteasomal protein degradation, we consider the evolution of the distribution $w(x|\tau)$ of the length x of the protein forward end beyond the first ring of the active sites at the discrete “time moment” τ . (Remember, τ is the number of the peptide bond near the first ring of cleavage centers, x and τ are integer.) On this way, we treat the shift of the protein strand into the proteasome for one amino acid (aa), i.e. the transition $\tau \rightarrow \tau + 1$. Let us decompose $w(x|\tau + 1)$ as

$$w(x|\tau + 1) = \sum_j w_j(x|\tau + 1),$$

where $w_j(x|\tau + 1)$ are the contributions due to different scenarios of this transition. Along with $w(x|\tau)$, we account $Q(n, m|\tau)$, the amount of the peptide (n, m) (where n and m denote the sequence position of the peptide within the initial substrate) generated during the transition $\tau \rightarrow \tau + 1$.

Here are three possible elementary events:

- (a) the strand shift: $x \rightarrow x + 1, \tau \rightarrow \tau + 1$. The probability of this event during the time unit (in other words, rate) is $v(x)$;
- (b) the cleavage on the first ring of cleavage centers ($x = 0$): $x \rightarrow 0, \tau \rightarrow \tau$. The event rate is $\gamma(\tau)$;
- (c) the cleavage on the second ring of cleavage centers ($x = L, L$ is the distance between the rings of cleavage centers): $x \rightarrow L, \tau \rightarrow \tau$. The event rate is $\gamma(\tau - L)$.

In terms of these elementary events the possible scenarios of the transition $\tau \rightarrow \tau + 1$ are

1) The elementary event (a). Its probability is

$$P_1(x|\tau) = \begin{cases} \frac{v(x)}{v(x) + \gamma(\tau)}, & x \leq L; \\ \frac{v(x)}{v(x) + \gamma(\tau) + \gamma(\tau - L)}, & x > L. \end{cases}$$

In this scenario, $x \rightarrow x + 1$, and

$$w_1(x + 1|\tau + 1) = P_1(x|\tau) w(x|\tau). \quad (9)$$

No peptides are generated.

2) The elementary event (b), which may not be followed by anything but the strand shift for one aa (as there is nothing to be cleaved). This scenario probability is

$$P_2(x|\tau) = \begin{cases} \frac{\gamma(\tau)}{v(x) + \gamma(\tau)}, & x \leq L; \\ \frac{\gamma(\tau)}{v(x) + \gamma(\tau) + \gamma(\tau - L)}, & x > L. \end{cases}$$

In this scenario, $x \rightarrow 1$, and

$$w_2(x|\tau + 1) = \delta_{x,1} \sum_{x'=1}^{\infty} P_2(x'|\tau) w(x'|\tau). \quad (10)$$

The peptides cut out are

$$Q_2(\tau, \tau - x + 1|\tau) = P_2(x|\tau) w(x|\tau). \quad (11)$$

3) The elementary event (c), which may be followed either by the strand shift (1) or by the scenario (2). The probability of the first stage (c) is

$$P_c(x|\tau) = \begin{cases} 0, & x \leq L; \\ \frac{\gamma(\tau - L)}{v(x) + \gamma(\tau) + \gamma(\tau - L)}, & x > L. \end{cases}$$

After the event (c), when $x \rightarrow L$, the number of the system states generated is

$$w_c(x|\tau) = \delta_{x,L} \sum_{x'=L+1}^{\infty} P_c(x'|\tau) w(x'|\tau),$$

and the peptides cut out are

$$Q_c(\tau - L, \tau - x + 1|\tau) = P_c(x|\tau) w(x|\tau).$$

The subsequent events (1) or (2) should be regarded as the corresponding above mentioned scenarios starting with the distribution $w_c(x|\tau)$, i.e.,

$$\begin{aligned} w_{c1}(x|\tau + 1) &= P_1(L|\tau) w_c(x - 1|\tau) \\ &= P_1(L|\tau) \delta_{x,L+1} \sum_{x'=L+1}^{\infty} P_c(x'|\tau) w(x'|\tau), \end{aligned} \quad (12)$$

$$\begin{aligned} Q_{c1}(\tau - L, \tau - x + 1|\tau) &= P_1(L|\tau) Q_c(\tau - L, \tau - x + 1|\tau) \\ &= P_1(L|\tau) P_c(x|\tau) w(x|\tau), \end{aligned} \quad (13)$$

$$\begin{aligned} w_{c2}(x|\tau + 1) &= \delta_{x,1} \sum_{x'=1}^{\infty} P_2(x'|\tau) w_c(x'|\tau) \\ &= \delta_{x,1} P_2(L|\tau) \sum_{x'=L+1}^{\infty} P_c(x'|\tau) w(x'|\tau), \end{aligned} \quad (14)$$

$$\begin{aligned} Q_{c2}(\tau - L, \tau - x + 1|\tau) &= P_2(L|\tau) Q_c(\tau - L, \tau - x + 1|\tau) \\ &= P_2(L|\tau) P_c(x|\tau) w(x|\tau). \end{aligned} \quad (15)$$

$$\begin{aligned} Q_{c2}(\tau, \tau - x + 1|\tau) &= P_2(x|\tau) w_c(x|\tau) \\ &= \delta_{x,L} P_2(L|\tau) \sum_{x'=L+1}^{\infty} P_c(x'|\tau) w(x'|\tau). \end{aligned} \quad (16)$$

Collecting the terms (9), (10), (12), (14), one finds

for $\underline{x = 1}$:

$$\begin{aligned} w(1|\tau + 1) &= w_2(1|\tau + 1) + w_{c2}(1|\tau + 1) \\ &= \sum_{x=1}^{\infty} \frac{\gamma_{\tau} w(x|\tau)}{v_x + \gamma_{\tau} + \Theta(x-L-1)\gamma_{\tau-L}} \\ &\quad + \frac{\gamma_{\tau}}{v_L + \gamma_{\tau}} \sum_{x=L+1}^{\infty} \frac{\gamma_{\tau-L} w(x|\tau)}{v_x + \gamma_{\tau} + \gamma_{\tau-L}}, \end{aligned} \quad (17)$$

for $\underline{1 < x \leq L+1}$:

$$w(x|\tau + 1) = w_1(x|\tau + 1) = \frac{v_{x-1} w(x-1|\tau)}{v_{x-1} + \gamma_{\tau}}, \quad (18)$$

for $\underline{x = L+1}$:

$$\begin{aligned} w(L+1|\tau + 1) &= w_1(L+1|\tau + 1) + w_{c1}(L+1|\tau + 1) \\ &= \frac{v_L}{v_L + \gamma_{\tau}} \left[w(L|\tau) + \sum_{x=L+1}^{\infty} \frac{\gamma_{\tau-L} w(x|\tau)}{v_x + \gamma_{\tau} + \gamma_{\tau-L}} \right], \end{aligned} \quad (19)$$

for $\underline{x > L+1}$:

$$w(x|\tau + 1) = w_1(x|\tau + 1) = \frac{v_{x-1} w(x-1|\tau)}{v_{x-1} + \gamma_{\tau} + \gamma_{\tau-L}}. \quad (20)$$

Here the Heaviside function $\Theta(x) = \begin{cases} 0 & \text{for } x < 0, \\ 1 & \text{for } x \geq 0. \end{cases}$ The system (17)–(20) is equivalent to the system (1)–(3) in the letter. In its turn, the whole contribution to the cleavage pattern

$$\begin{aligned} Q(\tau, \tau - x + 1|\tau) &= Q_2(\tau, \tau - x + 1|\tau) \\ &\quad + Q_{c2}(\tau, \tau - x + 1|\tau) \\ &= \frac{\gamma_{\tau} w(x|\tau)}{v_x + \gamma_{\tau} + \Theta(x-L-1)\gamma_{\tau-L}} \\ &\quad + \frac{\delta_{x,L} \gamma_{\tau}}{v_L + \gamma_{\tau}} \sum_{x_1=L+1}^M \frac{\gamma_{\tau-L} w(x_1|\tau)}{v_{x_1} + \gamma_{\tau} + \gamma_{\tau-L}}; \end{aligned} \quad (21)$$

$$\begin{aligned} Q(\tau-L, \tau-L-x+1|\tau) &= Q_{c1}(\tau-L, \tau-L-x+1|\tau) \\ &\quad + Q_{c2}(\tau-L, \tau-L-x+1|\tau) \\ &= \frac{\gamma_{\tau-L} w(L+x|\tau)}{v_{L+x} + \gamma_{\tau} + \gamma_{\tau-L}}. \end{aligned} \quad (22)$$

All the rest [not specified by the expressions (21), (22)] elements $Q(m, n|\tau)$ are zero. The expressions for the digestion pattern $Q(m, n)$ after a single polypeptide processing are different for short polypeptides and long ones of a periodic aa sequence.

Short (25–50 aa) synthetic polypeptides

For a short polypeptide of the length M , the releasing of the last fragment from the chamber at the “time moment” $\tau = M$ should be additionally taken into account: $Q(M, M - x + 1|M) \rightarrow Q(M, M - x + 1|M) + w(x|M)$. Hence, one obtains from (21), (22)

$$\begin{aligned} Q(\tau_1, \tau_2) &= Q(\tau_1, \tau_2|\tau_1) \\ &\quad + \Theta(M - \tau_1 - L) Q(\tau_1, \tau_2|\tau_1 + L) \\ &= \delta_{\tau_1, M} w(\tau_1 + L - \tau_2 + 1|M) \\ &\quad + \frac{\gamma_{\tau_1} w(\tau_1 - \tau_2 + 1|\tau_1)}{v_{\tau_1 - \tau_2 + 1} + \gamma_{\tau_1} + \Theta(\tau_1 - \tau_2 - L)\gamma_{\tau_1 - L}} \\ &\quad + \frac{\delta_{\tau_1 - \tau_2 + 1, L} \gamma_{\tau_1}}{v_L + \gamma_{\tau_1}} \sum_{x=L+1}^M \frac{\gamma_{\tau_1 - L} w(x|\tau_1)}{v_x + \gamma_{\tau_1} + \gamma_{\tau_1 - L}} \\ &\quad + \Theta(M - \tau_1 - L) \frac{\gamma_{\tau_1} w(\tau_1 + L - \tau_2 + 1|\tau_1 + L)}{v_{\tau_1 + L - \tau_2 + 1} + \gamma_{\tau_1 + L} + \gamma_{\tau_1}}, \end{aligned}$$

here $1 \leq \tau_2 \leq \tau_1 \leq M$. This is Eq.(5) in the letter.

Long periodic polypeptides

For a long polypeptide of a T -periodic aa sequence the peculiarity is that the fragment amount grows almost linearly with “time” τ as the polypeptide being processed. Hence,

$$\begin{aligned} Q_N(\tau_1, \tau_2) &\equiv \lim_{\tau \rightarrow \infty} \frac{1}{\tau} \sum_{\tau'=1}^{\tau} Q_N(\tau_1, \tau_2|\tau') \\ &= \frac{1}{T} \sum_{\tau'=1}^T Q_{N,T}(\tau_1, \tau_2|\tau') \\ &= \frac{1}{T} \left[\frac{\gamma_{\tau_1} w_{N,T}(\tau_1 - \tau_2 + 1|\tau_1)}{v_{\tau_1 - \tau_2 + 1} + \gamma_{\tau_1} + \Theta(\tau_1 - \tau_2 - L)\gamma_{\tau_1 - L}} \right. \\ &\quad + \frac{\delta_{\tau_1 - \tau_2 + 1, L} \gamma_{\tau_1}}{v_L + \gamma_{\tau_1}} \sum_{x=L+1}^{\infty} \frac{\gamma_{\tau_1 - L} w_{N,T}(x|\tau_1)}{v_x + \gamma_{\tau_1} + \gamma_{\tau_1 - L}} \\ &\quad \left. + \frac{\gamma_{\tau_1} w_{N,T}(\tau_1 + L - \tau_2 + 1|\tau_1 + L)}{v_{\tau_1 + L - \tau_2 + 1} + \gamma_{\tau_1 + L} + \gamma_{\tau_1}} \right], \end{aligned}$$

here $1 \leq \tau_2 \leq T$ and $\tau_1 \geq \tau_2$. This coincides with the expression (8) in the letter.